

# Structural transformation of collagen fibrils in corneal stroma during drying

## An x-ray scattering study

Peter Fratzl and Albert Daxer

Institut für Festkörperphysik der Universität Wien, Strudlhofgasse 4, A - 1090 Vienna, Austria and Universitätsklinik für Augenheilkunde, Anichstrasse 35, A - 6020 Innsbruck, Austria

**ABSTRACT** X-ray scattering experiments were performed on human corneas during drying. In a first stage the collagen interfibrillar distance decreased considerably. Then, at a critical point of dehydration, a structural transformation of the collagen fibrils was observed. This finding leads to a two-stage drying model, which explains the discrepancy between the collagen fibril diameters determined by x-ray scattering and by electron microscopy. Our results strongly suggest that the collagen fibrils in the corneal stroma are surrounded by a cylindrical coating made mainly of proteoglycans. The coating appears as a three-dimensional fractal network with fractal dimension of  $2.7 \pm 0.1$ .

### I. INTRODUCTION

The cornea is the anterior, projecting, and transparent part of the eye. The corneal stroma consists of layers of type I collagen fibrils. The ordering of the fibrils is thought to be responsible for the transparency of the tissue and their short-range ordered arrangement is well established (1–5).

X-ray scattering studies (6–8) as well as neutron scattering experiments (9) show changes in the collagen interfibrillar distance as a function of hydration state. The scattering pattern of the hydrated cornea consists of reflections from collagen interfibrillar distance and from higher orders of the well known 66 nm axial collagen period (6). The x-ray scattering pattern of collagen fibrils in the corneal stroma is very atypical with respect to other type I collagen tissues (e.g., tendon) because of the absence of the first-order reflection of the 66 nm period.

In a recent synchrotron x-ray diffraction study (10) the hydration dependence of the corneal structure was reinvestigated including low- as well as high-angle scattering data. Both, intermolecular and interfibrillar spacings of collagen were thus obtained as a function of hydration. The experimental data with respect to the hydration dependent variation of the interfibrillar distance were reported to differ significantly from the calculated values. It was found that, around physiological hydration, most of the water is taken up by the extrafibrillar substance, whereas at low hydration, the fibrils themselves also become dehydrated. The reason for this behavior is, however, still unknown.

To elucidate this question we have investigated the drying of the human corneas above and below a critical point of dehydration, using a small-angle x-ray scattering apparatus that allowed recording of low- and high-angle scattering data. A structural transformation of the

fibrils was found to take place at very low hydration and the corresponding x-ray scattering patterns are reported and discussed in this paper. As a result of this analysis a two-stage drying model is proposed for the cornea.

### II. MATERIALS AND METHODS

Human corneas were obtained within 5 hours after death. They were fully transparent and no lesion could be detected under the slit lamp microscope. Each cornea was dissected into several parts and stored in a 20 ml sterile chondroitin sulfate dextran corneal storage medium DEXSOL (CHIRON Ophthalmics, Irvine, CA, USA) under different temperature conditions ( $-80^{\circ}\text{C}$  to  $+5^{\circ}\text{C}$ ). Freezing was found to have no influence on the scattering pattern. The measurements were performed at room temperature. For some samples, epithelium and endothelium were removed by scraping with a scalpel before measurement. We found that this procedure had no detectable effect on the x-ray scattering pattern.

As usual (10), the water content of the sample was measured by means of the dimensionless parameter  $H$  defined as

$$H = (P/P_0) - 1 \quad (1)$$

where  $P$  is the weight of the cornea at hydration  $H$  and  $P_0$  is the weight after extensive vacuum drying. Starting from the physiological state, corneas were dried in an air flow at room temperature and weighted. Then they were enclosed into an air-tight container made of welded plastic sheets and mounted into the vacuum chamber of the x-ray scattering apparatus. After the measurement, the samples were dried in a vacuum chamber and weighted again to determine  $P_0$ .

For the measurements, we used a 12 kW x-ray generator and a pin-hole x-ray camera with variable distance (23–104 cm) from the sample to the detector. The detector was a SIEMENS two-dimensional position sensitive proportional counter (SIEMENS AG, Karlsruhe, Germany). The x-ray beam was directed parallel to the optical axis of the cornea. The two-dimensional spectra were corrected for parasitic pin-hole scattering and then radially averaged to give a scattering intensity  $I(k)$  as a function of

$$k = 4\pi/\lambda \sin(\theta/2) \quad (2)$$

where  $\lambda = 1.54 \text{ \AA}$  is the wavelength of the x-ray beam and  $\theta$  the scattering angle between the incident and the diffracted beam. The counting time for a x-ray spectrum was typically 20–30 min. Taking advantage of the variable sample to detector distance, a  $k$ -range from  $0.08$  to  $8 \text{ nm}^{-1}$  (including both interfibrillar and intermolecular reflections) was covered by each measurement.

Address correspondence to Dr. Albert Daxer, Universitätsklinik für Augenheilkunde, Anichstrasse 35, A-6020 Innsbruck, Austria.

The results were presented in abstract form at the IXth Congress of the European Society of Ophthalmology, Brussels, May 23–28, 1992.

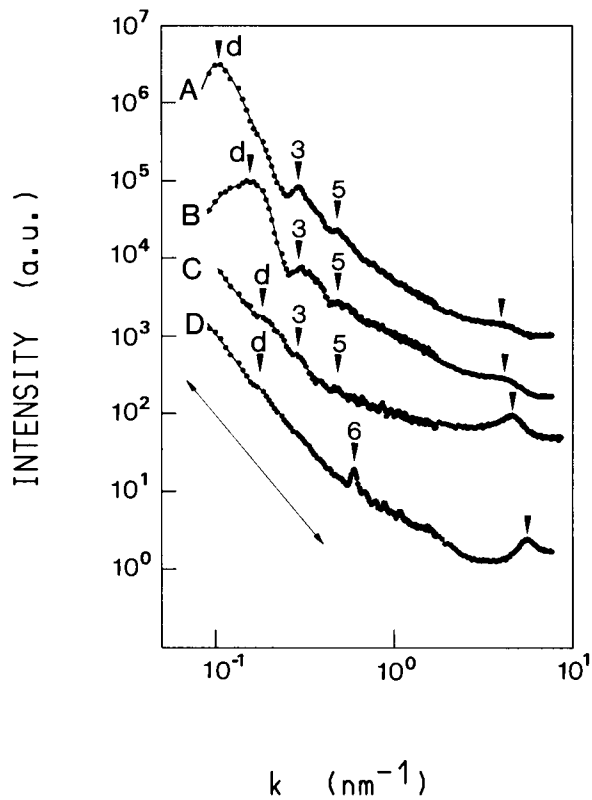


FIGURE 1 X-ray scattering curves  $I(k)$  in double-logarithmic scales for human cornea with (A)  $H = 4$ , (B)  $H = 1$ , (C)  $H = 0.5$ , and (D)  $H = 0$ . The incident x-ray beam was parallel to the optical axis of the cornea.  $k$  is the length of the scattering vector as defined in the text. The arrows labeled “3,” “5,” “6” indicate orders of the axial periodicity of type I collagen fibrils. The arrows labeled  $d$  show the position of the interference maximum due to the typical distance between neighboring collagen fibrils. The slope of the arrowed line below curve (D) is  $2.7 \pm 0.1$ . The unlabeled arrow corresponds to the intermolecular distance in the fibril.

Finally, it should be mentioned that some anisotropy of the scattering was observed in the 2-d spectra, indicating a tendency towards a preferential orientation of the fibrils into two directions perpendicular to each other. Similar patterns were also reported in earlier studies by x-ray and neutron scattering (7, 9).

### III. RESULTS

Typical scattering curves  $I(k)$  of the human cornea at four different states of hydration ( $H = 4$ ,  $H = 1$ ,  $H = 0.5$ ,  $H = 0$ ) are shown in Fig. 1. The small-angle as well as the wide-angle region can be seen. The maximum labeled  $d$  corresponds to the typical distance between collagen fibrils, the maxima labeled “3” and “5” are due to the internal structure of the fibrils and represent higher orders of the axial periodicity (10). The maxima “3” and “5” remain almost unchanged during the first stage of drying (between  $H = 4$  and  $H = 1$ ), which is known to be reversible (6, 7). A shoulder marked by unlabelled arrow in the region of large  $k$  is due to the intermolecular spacing in the collagen fibrils (10), see Fig. 1 curves A to

D. At a critical point of dehydration,  $H = 1$ , a structural transformation of the collagen fibril starts to take place and the scattering pattern changes in the following way (Fig. 1, curves C and D):

- i) Almost disappearance of the reflection due to the collagen interfibrillar distance ( $d$  in Fig. 1). This indicates that the electron density contrast between fibrils and interfibrillar substance has almost disappeared. Only a small shoulder remains in curves C and D, which is tentatively interpreted to be due to the interfibrillar distance.
- ii) The reflections representing the third (labeled “3”) and the fifth (labeled “5”) order of the axial 66 nm collagen period decrease strongly and finally disappear.
- iii) The reflection in the high angle region, due to the intermolecular spacing in the collagen fibrils (unlabeled arrows in Fig. 1) sharpens and shifts to larger  $k$ .
- iv) A completely new reflection (labeled “6” in Fig. 1) appears at hydration  $H = 0$ . The position of the peak corresponds exactly to the sixth order of the axial 66 nm period.
- v) At hydration  $H = 0$ , the small-angle scattering intensity  $I(k)$ ,—plotted in double logarithmic scales, is linear at small  $k$  with a slope of  $2.7 \pm 0.1$  (shown by the double arrow in Fig. 1).

### IV. TWO-STAGE DRYING MODEL

Below  $H = 1$  ( $H < 1$ ), the fibril diameter depends on  $H$  and the fibril structure changes (Fig. 1). For  $H > 1$  we found (in agreement with reference 10) that the intermolecular distance—and therefore the fibril diameter—stays approximately constant, whereas the interfibrillar distance depends on  $H$  (Fig. 1). It is, therefore, natural to propose a two-stage drying model, where it is assumed that the collagen fibrils have a much stronger affinity for water than the interfibrillar substance. For  $H > 1$ , water is released only by the interfibrillar substance. At  $H < 1$ , further drying is only possible by removing water from inside the fibril. Assuming that the swelling and shrinking occurs in the two-dimensional cross section perpendicular to the fibril direction (10), this model yields for the diameter  $D$  of the fibrils:

$$\begin{aligned} D^2 &= D_0^2 + (D_c^2 - D_0^2)H/H_0 \quad \text{for } H < H_c \\ D &= D_c \quad \text{for } H \geq H_c \end{aligned} \quad (3)$$

where  $D_0$  and  $D_c$  are the diameters at  $H = 0$  and  $H = H_c$ ,  $H_c = 1$  being the critical point of dehydration where the fibrils are saturated with water.

Assuming further a partial dissolution of the interfibrillar substance in water, the total volume of the cornea is  $V_t = V_0 + \mu V_w$ , where  $V_0$  is the volume of the dry cornea and  $V_w$  is the volume of water.  $\mu$  is a dimensionless coefficient which is 1 if there is no dissolution of the interfibrillar substance and smaller than 1 if there is partial dissolution. This leads to (using Eq. 1)

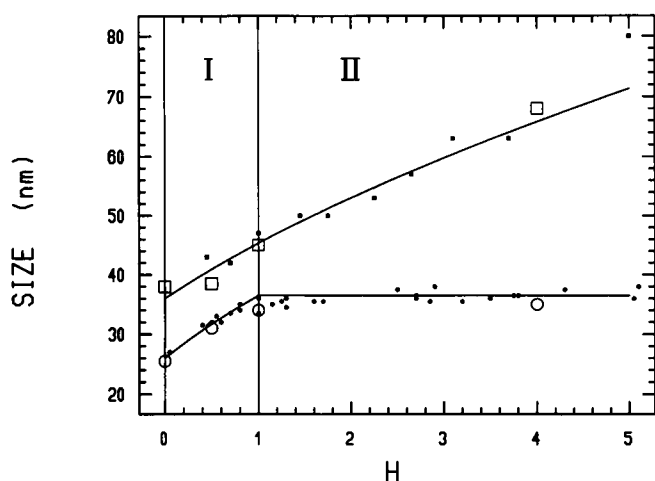


FIGURE 2 Interfibrillar distance  $d$  (upper curve) determined via Eq. 5 and fibril diameter  $D$  (lower curve) determined via Eq. 6. The small dots are data taken from reference 10, the large symbols correspond to data from Fig. 1.  $H$  is the hydration defined by Eq. 1. The full lines correspond to Eqs. 3 and 4. The roman numerals denote regions of the diagram corresponding to the two hydration stages discussed in the text.

$$d^2 = d_0^2(1 + \mu\rho_0 H) \quad (4)$$

where  $d_0$  is the value of the interfibrillar center-to-center distance  $d$  at  $H = 0$  and  $\rho_0 = 1.36$  the relative density of the dry cornea.

An equation corresponding to Eq. 4 with  $\mu = 1$  (i.e., no dissolution) has already been used (10). A comparison with experimental values for  $d$  showed that the increase of  $d$  is much smaller than predicted by Eq. 4 with  $\mu = 1$ . To explain this discrepancy, the formation of lakes at degrees of hydration (starting with  $H \geq 1$ ) was proposed (10), far below physiological hydration where lakes are not expected. Including the possibility of partial dissolution of interfibrillar substance in water, i.e., allowing  $\mu$  to be smaller than 1, the data can perfectly be reproduced by Eq. 4 without the assumption of lakes. This is shown in Fig. 2 where data for  $d$  are represented by squares (including data from the present work as well as from reference 10). The values for the interfibrillar distance  $d$  were determined from the x-ray spectra in the usual way (8, 10) assuming a hexagonal-like lattice:

$$d = 1.12(2\pi/k_m) \quad (5)$$

where  $k_m$  is the position of the corresponding peak in  $I(k)$ . The fit with Eq. 4 is shown in Fig. 2 by a full line. We obtain  $d_0 = 36$  nm and  $\mu = 0.43$ .

To perform a numerical comparison between our data and Eq. 3, it was necessary to convert the intermolecular spacing  $\delta$  (as determined from Bragg-positions, i.e., arrows in Fig. 1) into the fibril diameter  $D$ . If the geometry of the intermolecular arrangement is not perturbed too much in the drying process, both quantities should be proportional. If we estimate the proportionality constant, using the values in the dry state  $\delta_0$  and  $D_0$ , we get

$$D = \delta(D_0/\delta_0). \quad (6)$$

From Fig. 1  $D$  we have  $\delta_0 = 1.14$  nm and, taking for  $D_0$  the value determined by electron microscopy of dehydrated cornea (reference 11,  $D_0 = 26$  nm) we obtain the proportionality constant in Eq. 6.  $D$  is shown in Fig. 2 (circles) including data from this work and from Meek et al. (10). A fit of the data using Eq. 3 is shown by full line and yields  $D_c = 36.5$  nm for the fibril diameter in wet cornea. This is in excellent agreement with electron microscopy results of wet frozen corneas (12).

## V. DISCUSSION

The drying of cornea was found to proceed in two stages. Around physiological hydration (stage II in Fig. 2) only the interfibrillar substance is dehydrated. The fibril diameter is constant and equal to 36.5 nm.

At a critical point of dehydration ( $H = 1$ ), the interfibrillar substance has released all its water and the fibrils themselves are dehydrated, which finally leads to a structural transformation of the fibril (stage I in Fig. 2).

The reduction in the fibril diameter from stage II ( $H > 1$ ) to the dry state ( $H = 0$ ), corresponds exactly to the difference in the diameters seen in electron microscopy for physiologically hydrated low temperature treated samples (12) and for fixed and stained samples (11).

Therefore, if one assumes that the original electron micrographs of fixed and stained cornea samples (11) represent the fully dehydrated state, the results of x-ray scattering and electron microscopy are fully consistent.

If the fibrils were free to move inside the matrix consisting mainly of proteoglycans and water (in stage II), there should be some of the fibrils coming close enough to touch each other. It is, however, obvious in typical electron micrographs of transverse sections through the collagen fibril structure (11), that the fibrils do not come closer than a given distance. This is shown in Fig. 3, where the structure of rabbit cornea has been redrawn schematically from an electron micrograph (Fig. 3 *e* from reference 11). The region reproduced has a size of  $L \times L$ , where  $L = 0.25$   $\mu$ m. The black circles have a diameter of 26 nm, corresponding to the average value of the fibril diameter in the dry state ( $H = 1$ ).

Moreover the packing fraction  $\sigma = n\pi R_F^2$  (where  $n$  is the number of disks per unit surface and  $R_F$  the radius of the fibrils) of the disks corresponding to the cross sectional appearance of the collagen fibril (black disks in Fig. 3) is close to  $\sigma = 0.28$ . The x-ray scattering functions of liquid like arrangements of disks are well known (13), and for this packing fraction of 0.28 there is hardly a maximum in  $I(k)$ , in contrast to the observations by x-ray scattering (Fig. 1). Therefore, it is important to note that there is much more order in the structure of Fig. 3 than would be expected from a simple liquid of disks of diameter size of 26 nm. Drawing circles of diame-

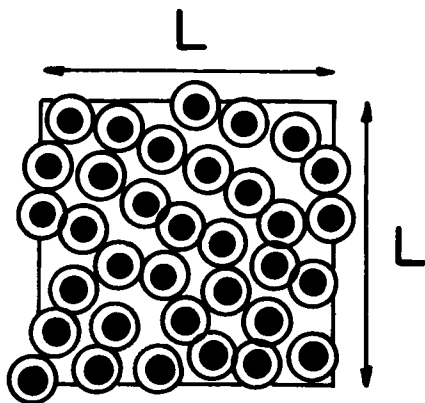


FIGURE 3 The black disks indicate the cross-section of fibrils with a radius  $R_F = 13$  nm, inside a box with side-length  $L = 0.25$   $\mu\text{m}$ . The position and the size ( $R_F = 13$  nm) of the fibrils have been taken from a portion of Fig. 3 *e* of reference 11. The open circles around each disk have a radius of  $R_C = 18.25$  nm.

ter 36.5 nm around each fibril (circles around the black disks in Fig. 3), there is practically no overlapping of those circles, but neighboring circles are now touching each other (Fig. 3).

These considerations strongly suggest that there is a coating around each fibril, which in the case of Fig. 3 has a diameter of 36.5 nm, preventing the fibrils to come closer than this distance. Presumably, this coating may be made mainly of proteoglycans known to bind at specific sites along the collagen fibril (14). Taking now the radius of the coated fibril  $R_C$  (18 nm) to calculate the packing fraction, one gets  $\sigma = 0.66$ , instead of 0.28 for the naked fibrils. The scattering function from a two-dimensional liquid with a packing fraction  $\sigma = 0.66$  is known to exhibit a fairly sharp peak at  $kR_C/\pi = 1$  (13), which produce a peak in  $I(k)$  close to  $k = 0.16$   $\text{nm}^{-1}$  for dehydrated cornea. This is exactly what we find by x-ray scattering (Fig. 1, peak *d* in curves *B–D*). The cross section as shown in Fig. 3 can, therefore, be understood as a liquid of hard disks, where the disks correspond to the coated fibrils. Twersky (15) has developed a model to explain the transparency of the cornea, where he assumed fibrils of a constant diameter surrounded by a coating of a diameter depending on the water content. This model corresponds exactly to what we observe in stage II of cornea hydration (see Fig. 2). We can therefore conclude that Twersky's model is not only capable of explaining the transparency of the tissue but also reflects the present x-ray scattering results.

Twersky's model, however, is not adequate anymore in stage I (see Fig. 2), because there, the fibrils are shrinking and the internal fibril structure is changed. This is reflected by the disappearance of the 3rd and 5th orders and the appearance of the 6th order of the axial collagen macroperiod. An enhancement of the 6th order also occurs upon drying of other type I collagen fibrils, like turkey tendon (16) but it is striking that, in the case

of cornea collagen, the 6th order dominates all others. This implies a periodicity of 11 nm, which corresponds to 39 residues, which is a typical repeat unit of charged amino acid residues on  $\alpha$ -chains (17). The reason for this structure change might be a breaking or rearrangement of collagen–proteoglycan bonds.

To complete this picture, it would be interesting to have more information on the structure of the coating. Some indications may, indeed, be gained from Fig. 1, in particular looking at curve *D*. In this curve, corresponding to a cornea vacuum-dried to an extent where the collagen has been structurally changed, there is still some x-ray scattering intensity at small values of  $k$ , although the interference peak “*d*” between the fibrils has almost disappeared. This intensity seems to be present also, as a background, below the interference maxima of curves *A* to *C*. It is probable, therefore, that this scattering is due to the interfibrillar substance. Moreover, this intensity is linear in double logarithmic scales (Fig. 1), which usually occurs for systems with fractal structure (18). Fractal structures are characterized by self-similar appearance of this picture when the magnification is changed. Fractal geometry is a powerful tool to characterize complex structures, like biological macromolecules (19). For a volume fractal of dimension  $D$ , the scattering intensity would behave like

$$I(k) = I_0 k^{-D} \quad (7)$$

where  $I_0$  is a constant. The slope of curve (*D*) in Fig. 1 (double arrowed line) would then correspond to a fractal dimension of  $D = 2.7 \pm 0.1$  (value  $\pm$  estimated error of the method) (Eq. 7) for the interfibrillar substance. A sketch of the structure of the coating is shown in Fig. 4.

## VI. CONCLUSION

An x-ray scattering investigation of the drying process of cornea has shown that the dehydration of the cornea occurs in two stages. In stage II (physiological hydration) the collagen fibril diameters stay constant and drying is due to water release by the interfibrillar substance. The structure of the cornea in stage II may be best described by Twersky's model (15), where cylindrical collagen fibrils of constant size are supposed to be surrounded by a cylindrical coating of variable size made essentially by proteoglycans attached to the fibril. There is some evidence from the x-ray scattering spectra that the coating is formed by a fractal network with dimension  $2.7 \pm 0.1$ . Below a critical point of dehydration ( $H = 1$ ), the fibrils themselves start to be dehydrated, presumably because the coating has released all its water (stage I). The drying of the collagen fibrils is accompanied by a structural change, which is characterized by a disappearance of the 3rd and the 5th order of the axial collagen macroperiod and by the appearance of a new periodicity with an 11 nm repeat unit.

Finally, the two-stage drying model removes the inconsistency between the experimental determined

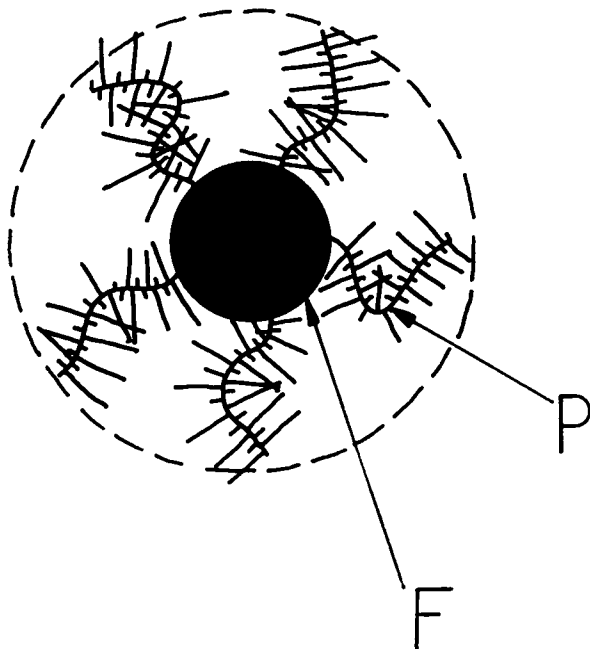


FIGURE 4 Model of the structure of the coated collagen fibril (F) in corneal stroma. The coating consists of a network of mainly proteoglycans (P) attached with one end to the fibril and forming a porous network with fractal dimension. It is capable of absorbing large quantities of water and of increasing in volume with increasing water content. The broken line indicates the outer limit of the coating. The diameter of this circle may vary between 36.5 and 80 nm, depending on the degree of hydration. The diameter of the fibril is typically 26 nm in the dry state, and may increase as described by the two-stage drying model in the text.

changes in interfibrillar spacing as a function of corneal hydration and the related theoretically predicted values by allowing partial dissolution of the interfibrillar substance. It also gives a simple explanation for the discrepancies usually observed for collagen fibril radii in cornea, as determined by x-ray scattering and by electron-microscopy.

Received for publication 25 August 1992 and in final form 18 November 1992.

## REFERENCES

1. Maurice, D. M. 1957. The structure and transparency of the corneal stroma. *J. Physiol.* 136:263–286.
2. Hart, R. W., and R. A. Farrell. 1969. Light scattering in the cornea. *J. Opt. Soc. Am.* 59:766–774.
3. Feuk, T. 1970. On the transparency of the stroma in the mammalian cornea. *IEEE Trans. Bio-Med. Eng.* 17:186–190.
4. Benedek, G. B. 1971. Theory of transparency of the eye. *Appl. Opt.* 10:459–473.
5. Farrell, R. A., R. L. McCally, and P. E. R. Tatham. 1973. Wavelength dependencies of light scattering in normal and cold swollen rabbit corneas and their structural implications. *J. Physiol.* 233:589–612.
6. Goodfellow, G. M., G. F. Elliott, and A. E. Woolgar. 1978. X-ray diffraction studies of the corneal stroma. *J. Mol. Biol.* 119:237–252.
7. Sayers, Z., M. H. J. Koch, S. B. Whitburn, K. M. Meek, G. F. Elliott, and A. Harmsen. 1982. Synchrotron x-ray diffraction study of corneal stroma. *J. Mol. Biol.* 160:593–607.
8. Worthington, C. R., and H. Inouye. 1985. X-ray diffraction study of the cornea. *Int. J. Biol. Macromol.* 7:2–8.
9. Elliott, G. F., Z. Sayers, and P. A. Timmins. 1982. Neutron diffraction studies of the corneal stroma. *J. Mol. Biol.* 155:389–393.
10. Meek, K. M., N. J. Fullwood, P. H. Cooke, G. F. Elliott, D. M. Maurice, A. J. Quantock, R. S. Wall, and C. R. Worthington. 1991. Synchrotron x-ray diffraction studies of the cornea, with implications for stromal hydration. *Biophys. J.* 60:467–474.
11. Craig, A. S., and D. A. D. Parry. 1981. Collagen fibrils of the vertebrate corneal stroma. *J. Ultrastruct. Res.* 74:232–239.
12. Craig, A. S., J. G. Robertson, and D. A. D. Parry. 1986. Preservation of corneal collagen fibril structure using low temperature procedures for electron microscopy. *J. Ultrastruct. Res.* 96:172–175.
13. Woodhead-Galloway, J., and P. A. Machin. 1976. X-ray scattering from a gas of uniform hard disks using the Percus-Yevick approximation: an application to a 'planar liquid'. *Mol. Phys.* 32:41–48.
14. Scott, J. E. 1988. Proteoglycan-fibrillar collagen interactions. *Biochem. J.* 252:313–323.
15. Twersky, V. 1975. Transparency of pair-related, random distributions of small scatterers, with applications to the cornea. *J. Opt. Soc. Am.* 65:524–530.
16. Fratzl, P., N. Fratzl-Zelman, and K. Klaushofer. 1993. Collagen packing and mineralization: An x-ray scattering investigation of turkey leg tendon. *Biophys. J.* 64:260–266.
17. Doyle, B. B., D. J. S. Hulmes, A. Miller, D. A. D. Parry, K. Piez, and J. Woodhead-Galloway. 1974. Axially projected collagen structures. *Proc. Roy. Soc. B.* 187:37–46.
18. Schmidt, P. W. 1989. In *The Fractal Approach to Heterogeneous Chemistry*, D. Avnir Editor. John Wiley and Sons Inc., New York. chap. 2.2.
19. Goetze, T., and J. Brickmann. 1992. Self similarity of protein surfaces. *Biophys. J.* 61:109–118.